Utilization of Nanoclay to Reinforce Flax Fabric-Geopolymer Composites

H. Assaedi, F. U. A. Shaikh, I. M. Low

Abstract—Geopolymer composites reinforced with flax fabrics and nanoclay are fabricated and studied for physical and mechanical properties using X-Ray Diffraction (XRD), Fourier Transform Infrared Spectroscopy (FTIR), and Scanning Electron Microscope (SEM). Nanoclay platelets at a weight of 1.0%, 2.0%, and 3.0% were added to geopolymer pastes. Nanoclay at 2.0 wt.% was found to improve density and decrease porosity while improving flexural strength and post-peak toughness. A microstructural analysis indicated that nanoclay behaves as filler and as an activator supporting geopolymeric reaction while producing a higher content geopolymer gel improving the microstructure of binders. The process enhances adhesion between the geopolymer matrix and flax fibres.

Keywords—Flax fibres, geopolymer, mechanical properties, nanoclay.

I. INTRODUCTION

GEOPOLYMERS are inorganic polymers formed through a polymerization process of aluminosilicate with alkaline solutions. Geopolymers possess a number of positive attributes in terms of flexural strength, elastic modulus with low shrinkage [1]. However, geopolymers tend to suffer as other ceramics from brittle breakdown. This limitation may be readily overcome with fibre reinforcement as in high performance polymer/matrix composites. Hitherto, the most common fibre reinforcements used in geopolymer composites have been based on carbon, basalt, glass and polyvinyl alcohol fibres [2], [3].

Due to environmental concerns, there is interest in replacing synthetic fibres with more natural fibres [4]. Natural plant fibres offer an advantage over synthetics fibres. The advantages are lower density, lower cost, biodegradable, specified properties, lower processing wear and lower energy consumption during the extraction process. The availability of natural fibres adds to the benefit for manufacturers of composites. Flax fibre is a main natural fibre that made up of 64.1% cellulose, 16.7% hemicelluloses, 1.8% pectin, and 2% lignin. FF also contains minor amounts of waxes, bound water, and inorganic component material [5]. In previous work, flay ash based geopolymer has been reinforced with flax fabrics, resulting in significant improvement on the mechanical properties of the eco-composites [6].

H. Assaedi is with the Department of Imaging & Applied Physics, Curtin University, GPO Box U1987, Perth, WA 6845, Australia (e-mail: hassaedi@gmail.com).

F. U. A. Shaikh is with the Department of Civil Engineering, Curtin University, GPO Box U1987, Perth, WA 6845, Australia.

I. M. Low is with the Department of Imaging & Applied Physics, Curtin University, GPO Box U1987, Perth, WA 6845, Australia.

Researchers of polymers and ceramics have recently become interested in nanotechnology, particularly in developing nanocomposites, which have superior physical and mechanical properties. A number of nanoparticles are being added to geopolymers to increase mechanical properties. For example, nanoalumina and nanosilica have been used successfully as reinforcements for geopolymer pastes, providing outstanding mechanical properties. The nanoparticles not only performed as voids-fillers, but also enhanced the geopolymer reaction [7]. In another study, it has been found that nanosilica and nanoalumina particles have the ability to reduce the porosity and water absorption of geopolymer matrices [8]. A further study on the effect of addition of carbon nanotubes to fly-ash-based geopolymer has shown an increase in the mechanical and electrical properties of geopolymer nanocomposites when compared to the control paste [9]. In another study, the addition of calcium carbonate ($CaCO_3$) nanoparticles to high-volume fly-ash concrete improved the flexural and mechanical properties, decreased the porosity, and improved the concrete resistance to water absorption [10]. Finally, in a more recent study of nanoclay cement nanocomposites, it was observed that nanoclay not only increased mechanical and physical properties of cement matrices, but also improved thermal properties [4]. However, no research is reported on the effect of nanoclay on properties of flax fabric reinforced geopolymer composites. Nanoclay as a semi-crystalline particle could play two roles: 1- as pore filling particles, 2- as activator for geopolymerisation reaction since the nanoplatelets are partially amorphous, and has high surface-to-volume ratio. This makes nanoclay a multifunctional filler to reinforce the geopolymer matrix.

In this study, the fabrication of eco-nano-composites using nanoclay and flax fibre (FF) as reinforcement of fly ash geopolymer matrices is investigated. Fourier Transform Infrared Spectroscopy (FTIR) and Scanning Electron Microscopy (SEM) are used to investigate the morphology and microstructure of geopolymer/flax nanocomposites. The effect of different nanoclay particles contents on physical and mechanical properties is also evaluated in this paper.

II. EXPERIMENTAL METHODS

A. Materials and Fabrication

Low calcium fly ash (ASTM class F), collected from the Eraring power station in NSW, and was used as the source material for the geopolymer matrix. The chemical composition of fly ash is shown in Table I. The alkaline activator for geopolymerisation was a combination of sodium hydroxide and sodium silicate grade D solution. Sodium hydroxide flakes

of 98% purity were used to prepare the solution. The chemical composition of sodium silicate used was 14.7% Na_2O, 29.4% SiO_2 and 55.9% water by mass.

TABLE I
CHEMICAL COMPOSITION OF FLY-ASH (WT%)

SiO_2	Al_2O_3	CaO	Fe_2O_3	K_2O	MgO	Na_2O
63.13	24.88	2.58	3.07	2.01	0.61	0.71
P_2O_5	SO_3	TiO_2	MnO	BaO	LOI	
0.17	0.18	0.96	0.05	0.07	1.45	

Flax fabric (FF) and organo-clay (Cloisite 30B) were used for the reinforcement of geopolymer nanocomposites. The fabric of 30×30 cm^2, supplied by Pure Linen Australia, is made up of yarns with a density of 1.5 g/cm^3; the space between the yarns is between 2 and 4 mm, necessary to allow the geopolymer matrix to penetrate. The average diameter of the fibre yarns was 0.60 mm, and the fibres diameter was about 20 μm. The nanoclay platelets used in this study was based on natural montmorillonite clay $(Na,Ca)_{0.33}(Al,Mg)_2(Si_4O_{10})(OH)_2.nH_2O)$ which was supplied by Southern Clay Products, USA. The description and physical properties of Cloisite 30B are shown in Table II.

TABLE II
PHYSICAL PROPERTIES OF THE NANOCLAY PLATELETS (CLOISITE 30B)

Colour	Off white
Density (g/cm^3)	1.98
d-spacing (001) (nm)	1.85
Aspect ratio	200-1000
Surface area (m^2/g)	750
Typical dry particle sizes:	90% volume < 13 μm
	50% volume < 6 μm
	10% volume < 2 μm

To prepare the geopolymer matrix, an alkaline solution to fly ash ratio of 0.75 was used and the ratio of sodium silicate solution to sodium hydroxide solution was fixed at 2.5. The concentration of sodium hydroxide solution was 8 M, and was prepared and combined with the sodium silicate solution one day before mixing.

The nanoclay was added first to the fly ash at the dosages of 0%, 1.0%, 2.0%, and 3.0% by weight. The fly ash and nanoclay were dry mixed for 5 min in a covered mixer at a low speed and then mixed for another 10 min at high speed until homogeneity was achieved. The alkaline solution was then added gradually to the fly ash/nanoclay in the mixer at a low speed until the mix became homogeneous, then further mixed for another 10 min on high speed. The resultant mixture was then poured into wooden moulds and placed on a vibration table for two minutes.

Similar mixtures were followed to produce the eco-nanocomposites. Four samples of geopolymer pastes reinforced with 4.1 wt% FF were prepared by spreading a thin layer of geopolymer paste in a well-greased wooden mould and carefully placing the first layer of FF on it. The fabric was fully saturated with paste by a roller, and the process repeated for ten layers; each specimen contained a different weight ratio of nanoclay (Table III). The samples then were left under

heavy weight for 1 hour to reduce entrapped air inside the samples. All samples were covered with plastic film and cured at 80°C for 24 hours in an oven before demoulding. They were then dried under ambient conditions for 28 days.

TABLE III
FORMULATION OF SAMPLES

Sample	Flyash (g)	NaOH (g)	Na_2SiO_3 (g)	Nanoclay	FF (wt%)
GPNC-0	1000	214.5	535.5	0	0
GPNC-1	1000	214.5	535.5	10	0
GPNC-2	1000	214.5	535.5	20	0
GPNC-3	1000	214.5	535.5	30	0
GPFNC-0	1000	214.5	535.5	0	4.1
GPFNC-1	1000	214.5	535.5	10	4.1
GPFNC-2	1000	214.5	535.5	20	4.1
GPFNC-3	1000	214.5	535.5	30	4.1

B. Characterization

The samples were measured on a D8 Advance Diffractometer (Bruker-AXS) using copper radiation and a LynxEye position sensitive detector. The diffractometer were scanned from 7° to 60° (2θ) in steps of 0.015° using a scanning rate of 0.5°/min. XRD patterns were obtained by using Cu Kα lines (k = 1.5406 Å). An FTIR spectrum was performed on a Perkin Elmer Spectrum 100 FTIR spectrometer in the range of 500-4000 cm^1 at room temperature. The spectrum was an average of 10 scans at a resolution of 2 cm^{-1}, corrected for background. The microstructures of geopolymer composites were examined using a Zeiss Neon focused ion beam scanning electron microscope (FIB–SEM), equipped with energy dispersive spectroscopy (EDS). The specimens were mounted on aluminium stubs using carbon tape and then coated with a thin layer of platinum to prevent charging before the observation.

C. Physical Properties

Measurements of bulk density and porosity were conducted to define the quality of geopolymer nanocomposite. Density of samples (ρ) with volume (V) and dry mass (md) was calculated using (1):

$$\rho = \frac{m_d}{V} \qquad (1)$$

The value of apparent porosity (P_a) was determined using Archimedes' principle in accordance with the ASTM Standard (C-20) [11]. Pure geopolymer and nanocomposite samples were immersed in clean water, and the apparent porosity (P_a) was calculated using (2):

$$P_a = \frac{m_a - m_d}{m_a - m_w} \times 100 \qquad (2)$$

where (m_a) is mass of the saturated samples in air, and (m_w) is mass of the saturated samples in water.

For the water absorption test, samples of pure geopolymer and geopolymer nanocomposites were dried at a temperature of 80°C until reaching stable mass (m_o). The samples were then submerged in clean water at a temperature of 20°C for 48 h. After the desired absorption period, the samples were

removed and the mass was weighed (m_1) immediately. The water absorption (W_A) of samples was calculated using:

$$W_A = \frac{m_1 - m_o}{m_o} \times 100 \qquad (3)$$

D. Mechanical Properties

A LLOYD Material Testing Machine (50kN capacity) with a displacement rate of 1 mm/min was used to perform the mechanical tests. Rectangular bars of $60 \times 18 \times 15$ mm^3 with a span of 40mm were cut from the fully cured samples for three-point bend tests to evaluate the mechanical properties. All samples were aligned horizontally to the applied load in all mechanical tests. Five samples of each composite were used to evaluate the flexural strength according to the standard ASTM D790 [12]. The values were recorded and analysed with the

machine software (NEXYGENPlus) and average values were calculated. The post-peak toughness is evaluated as the area under the load-midspan deflection curve beyond the peak point.

III. RESULTS AND DISCUSSION

A. X-Ray Diffraction (XRD)

The XRD spectra obtained for nanoclay, fly ash, GPNC-0, GPNC-1, GPNC-2 and GPNC-3 samples are given in Figs. 1 (a), (b). The crystalline phases were indexed using Powder Diffraction Files (PDFs) from the Inorganic Crystal Structure Database (ISCD).
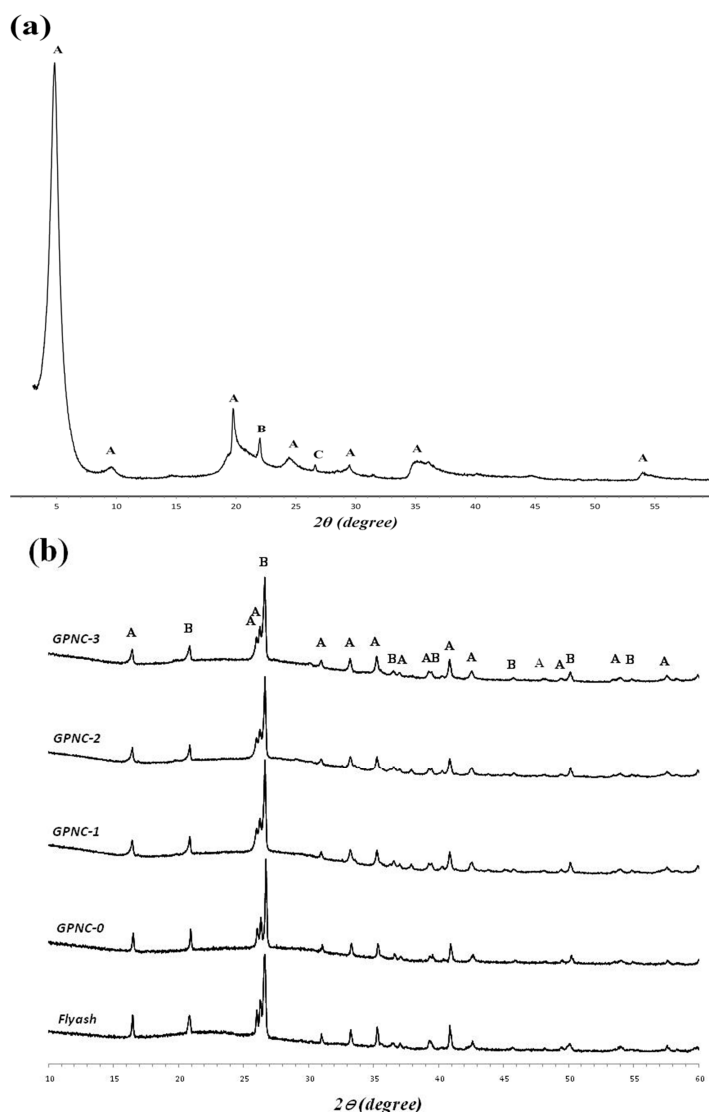

Fig. 1 (a) X-ray diffraction pattern of nanoclay (Cloisite 30B), (b) X-ray diffraction patterns of fly-ash, Geopolymer and geopolymer nanocomposites. Letters indicate: A=Cloisite 30B, B=Cristobalite, C=Quartz

The diffraction patterns of nanoclay are shown in Fig. 1 (a). Three phases have been indexed in the diffraction pattern of nanoclay with the major phase being Cloisite30B and minor phases of Cristobalite [SiO_2] (PDF 00-039-1425) and Quartz [SiO_2] (PDF 00-047-0718). Cloisite30B consists of Montmorillonite [$(Ca,Na)_{0.3}Al_2(Si,Al)_4O_{10}(OH)_2 \cdot xH_2O$] and the quaternary ammonium salt. Montmorillonite has four major peaks in the XRD pattern, which correspond to 2θ of 4.84°, 19.74°, 35.12° and 53.98°. The quaternary ammonium salt has four peaks at 2θ of 4.84°, 9.55°, 24.42° and 29.49°. Note that there is an overlap of peaks at 2θ of 4.84° for Montmorillonite and quaternary ammonium salt. Both Cristobalite and Quartz has a peak that corresponds to 2θ of 21.99° and 26.61°, respectively. Cloisite30B is semi-crystalline and partially amorphous material. Considering the diffraction pattern, most of the peaks are broad, which indicates small crystallite size and partially amorphous content.

For fly ash, GP and geopolymer nanocomposites samples, two major phases are identified clearly: quartz [SiO_2] (PDF 00-046-1045) and mullite [$Al_{1.272}Si_{0.278}O_{4.864}$] (PDF 01-083-1881) (Fig. 1 (b)). As the crystalline phases of quartz and mullite are also the fly ash phases they are insensitive to geopolymetric reactions, and their role is limited in geopolymer paste as filler particles [13], [14]. However, the amorphous aluminosilicate hump that created between $2\theta = 14°$ and $27°$ is an active signal of geopolymerisation. The amorphous content in the fly ash is the reactive and dissolvable content in alkaline solution throughout the geopolymer formation [15]. The physical and mechanical properties of geopolymer pastes are remarkably affected through the amorphous phase. When the amorphous phase is high, the strength of the geopolymer is likewise high [16], [17].

B. Fourier Transform Infrared Spectroscopy (FTIR)

The strong peaks at ~1000 cm^{-1} in geopolymer samples is associated with Si-O-T (T: Si or Al) asymmetric stretching vibrations and is the fingerprint of the geopolymerisation [18].

Fig. 2 shows an overlap of geopolymer special peak for pure geopolymer and nanocomposites. The level of geopolymerization can be identified quantitatively by comparing the height and the area under the geopolymer stretching peaks of the nanocomposites to the pure matrix peak [19]. Considering the size of the geopolymer peak, it can be seen that all nanocomposites had generally higher contents of geopolymer gel compared to the control paste; however, the loading of 2.0 wt.% of nanoclay had the highest level of geopolymerization among all samples. The areas under the geopolymer peak for the nanocomposites when compared to the pure matrix have enlarged by 2.0%, 7.0% and 3.0%, while the peak's heights have expanded by 2.0%, 19% and 15% for GPNC-1, GPNC-2 and GPNC-3, respectively.

C. Density, Porosity and Water Absorption

Water absorption and porosity results are shown in Fig. 3. Generally, composites that have been reinforced with FF display higher water absorption and porosity compared with samples that do not use FF. This is due to the hydrophilic nature of cellulose fibres, which creates voids between matrices and FF in interfacial regions [20]. Geopolymer nanocomposites samples displayed lower porosities and higher densities compared with control paste. Nanoclay particles indicate playing a pore-filling action, which reduces the porosity in geopolymer composites resulting in denser geopolymer matrices. The optimum loading was found as 2.0 wt% of nanoclay, which reduced the porosity by 7.1%, and the water absorption by 17% when compared to the pure geopolymer matrix. However, the addition of excessive amounts of nanoclay increased the porosity and water absorption, and decreased the density of the nanocomposite sample due to the poor dispersion and agglomeration of nanoparticles. This is a common phenomenon for nanoparticles due to their van der Waal's forces due to small sizes and high surface area to volume ratio of nanoparticles [21]. In eco-nanocomposites, physical properties were shown to exhibit a similar trend to nanocomposites. Optimum loading amount of nanoclay to eco-nanocomposites was observed in GPFNC-2, decreased value in porosity 16.3% and absorption of water by 19.4% lower than eco-composite (GPFNC-0).
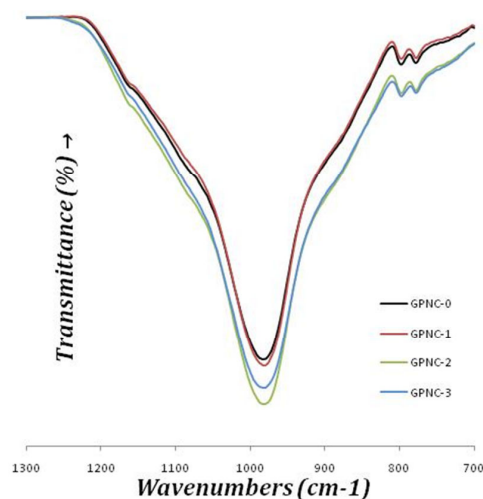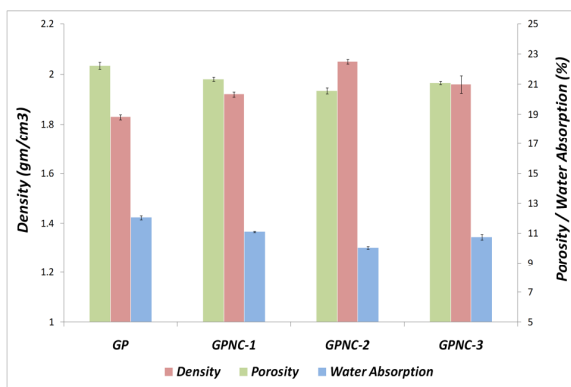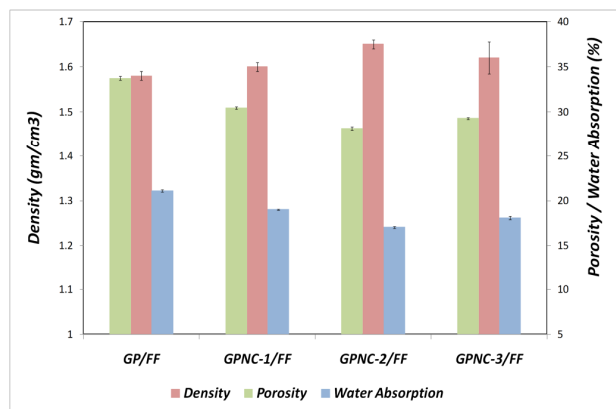

Fig. 2 FTIR scans for pure geopolymer and geopolymer nanocomposites

(b)

(b)

Fig. 3 (a), (b) Density, porosity, and water absorption for geopolymer eco-composite and geopolymer eco-nanocomposites

D. Mechanical Properties

Flexural tests are used to characterize the mechanical properties of layered composites as they offer a simple means of the bending response. This provides useful information on the performance of layered fabric-based composites. Figs. 4 and 5 show flexural strength and load-midspan deflection curves for control geopolymer paste, nanocomposites, FF-reinforced geopolymer composites and FF-reinforced nanocomposites.

It can be observed that in composites reinforced with FF displayed, in general, higher flexural strength than nanocomposites and pure geopolymer sample. Flexural strength showed improvement from 4.5 MPa in control samples to 23 MPa showed in GPFNC-0. The result is comparable to the flexural strength of geopolymer composites reinforced with short flax fibres [22]. This can be described by the fact that flax fibres bridged the cracks of geopolymer matrix during bending and resisted the failure through frictional deboning of fabric in the matrix. This allowed more stress transfer between the matrix and the flax fibres, resulting in greater flexural strength [23].
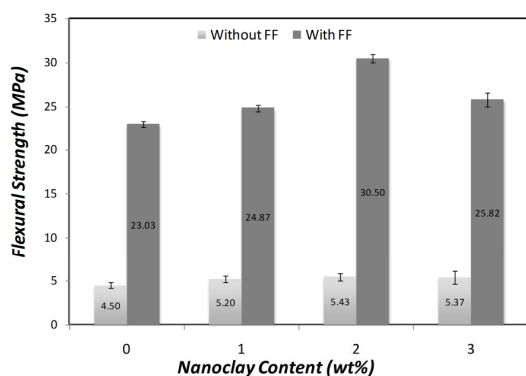

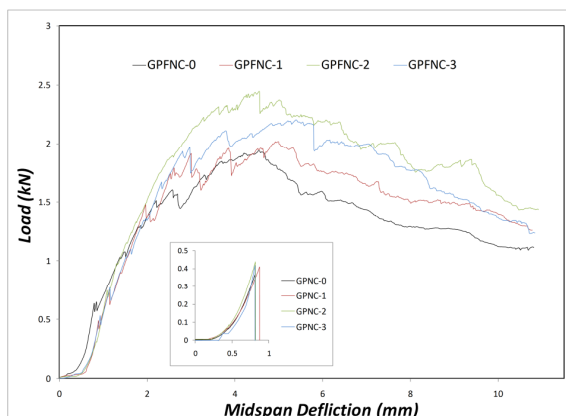Fig. 4 Flexural strength for all samples

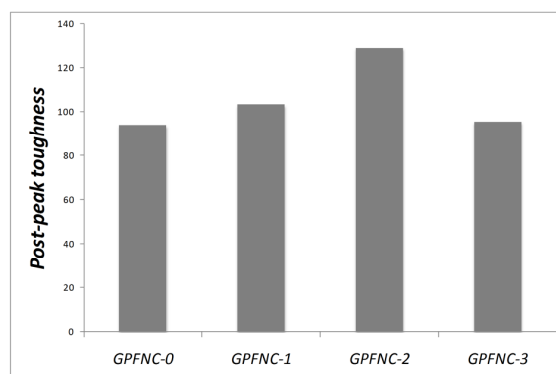Fig. 5 Load-midspan deflection curves for all samples

Fig. 6 Post-peak toughness for all samples

The flexural strengths of the pastes that reinforced with both FF and nanoclay particles were significantly improved due to the improvement of the physical structures of geopolymer matrices. The addition of nanoclay created denser matrices and enhanced adhesion bond between the fibres and matrix creating an eco-nanocomposites with superior mechanical properties. GPFNC-2 samples exhibited the highest flexural strength among all samples, which means that the optimal addition that improved the mechanical properties was 2.0 wt.% of nanoclay.

This result is also confirmed by studying post-peak toughness of the composites (Fig. 6). It can be seen that neat geopolymer and geopolymer nanocomposites had zero values of toughness because of the brittleness of the geopolymer. However, FF-reinforced composites showed higher post-peak toughness because of the ability of long fibres to withstand a greater load and to support multiple cracks during the loading process, which avoided the brittle failure of geopolymer. The sample loaded with the optimum addition of nanoclay and reinforced with flax fibres gave the highest toughness compared to other eco-nanocomposites. It might be worth to mention here that the effect of fibre pull-out occurred more extensively in GPFNC-0, GPFNC-1 and GPFNC-3 than in GPFNC-2. This may be attributed to the point that the bond between the matrix and flax fibres has improved due to the high content of geopolymer gel, which caused more fibres

fracture than the pull-out in GPFNC-2. This can be considered clearly in Fig. 5, where the slope of GPFNC-2 curve has sharper decrease in load with increasing deflection in the region between 9 and 11 mm than other curves.

IV. MICROSTRUCTURE ANALYSIS

Figs. 7 (a)–(d) show the SEM micrographs of fracture surface of neat geopolymer and geopolymer nanocomposites containing 1.0, 2.0, and 3.0 wt% nanoclay. The neat geopolymer has high porosity matrix and high number of non-reacted and partially reacted fly-ash particles embedded in the matrix (Fig. 7 (a)). For the 1–3 wt% nanoclay (Figs. 7 (b)–(d)) less numbers of fly-ash particles were observed, and the matrix appeared denser than that of the pure paste. Figs. 7 (e)-(f) show observation of the geopolymer matrices that loaded with 3.0 wt% nanoclay at low and high magnification. Nanoclay particles are poorly dispersed and agglomerated due to the high content of the nanoparticles.

SEM images of the fracture surface of FF-reinforced geopolymer eco-composite and eco-nanocomposite after bending tests are shown in Figs. 7 (g)-(h). Different toughness mechanisms such as fibre de-bonding, fibre pull-out and rupture and matrix fracture can be clearly seen. The examination of fracture surface of FF reinforced geopolymer eco-composite shows high porous structure and number of unreacted fly ash, which caused poor adhesion between fibres and the matrix (Fig. 7 (g)). However, In FF reinforced geopolymer containing 2.0 wt% nanoclay, less numbers of unreacted fly ash particles were observed, and higher content of geopolymer gel can be clearly seen, which provided better adhesion between the flax fibres and the matrix. Because of this, fibres fracture (Fig. 7 (h)) was investigated rather than pull-out in nanocomposites loaded with the optimal addition of nanoparticles.
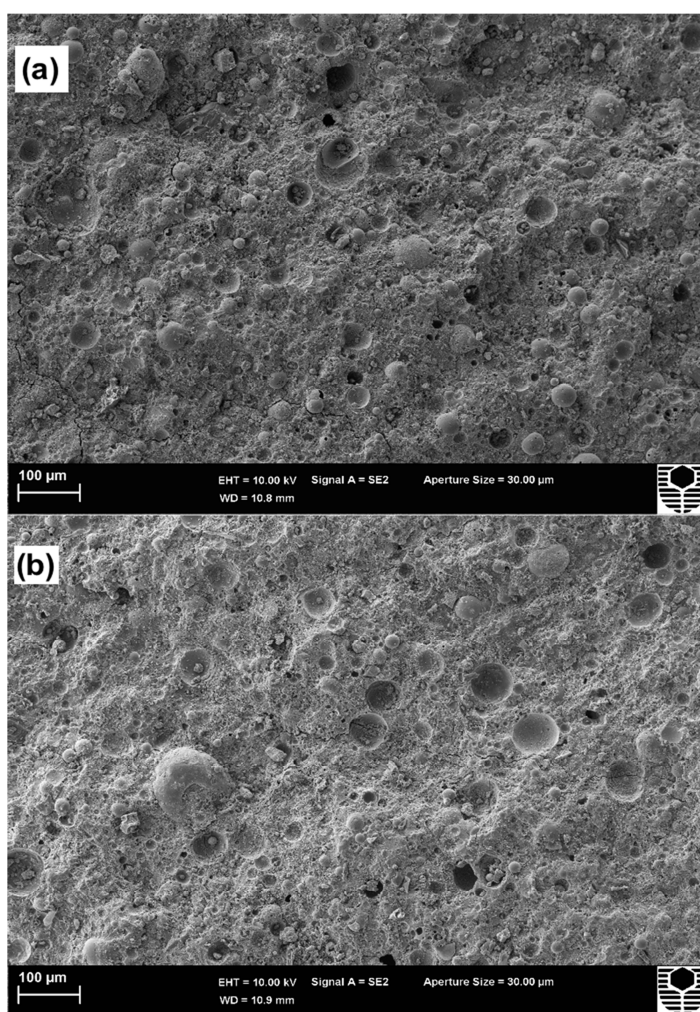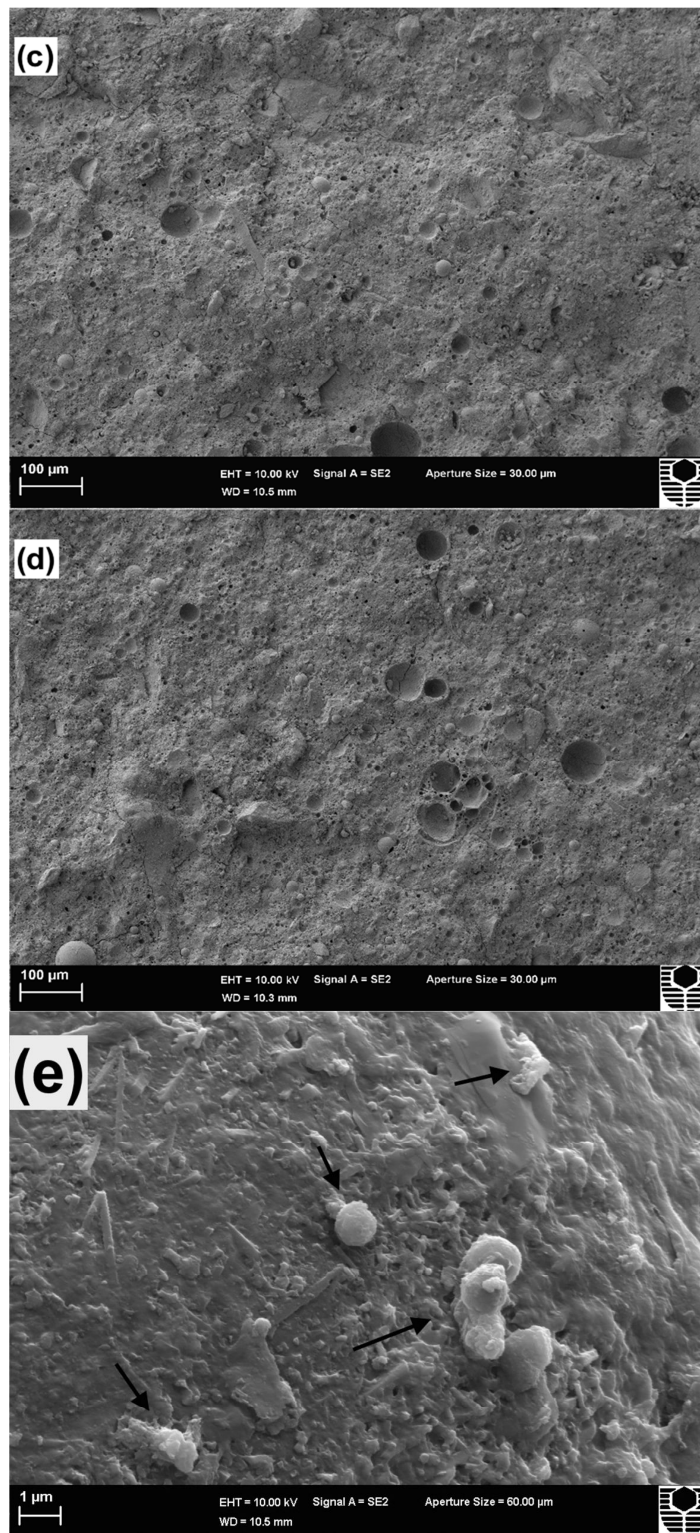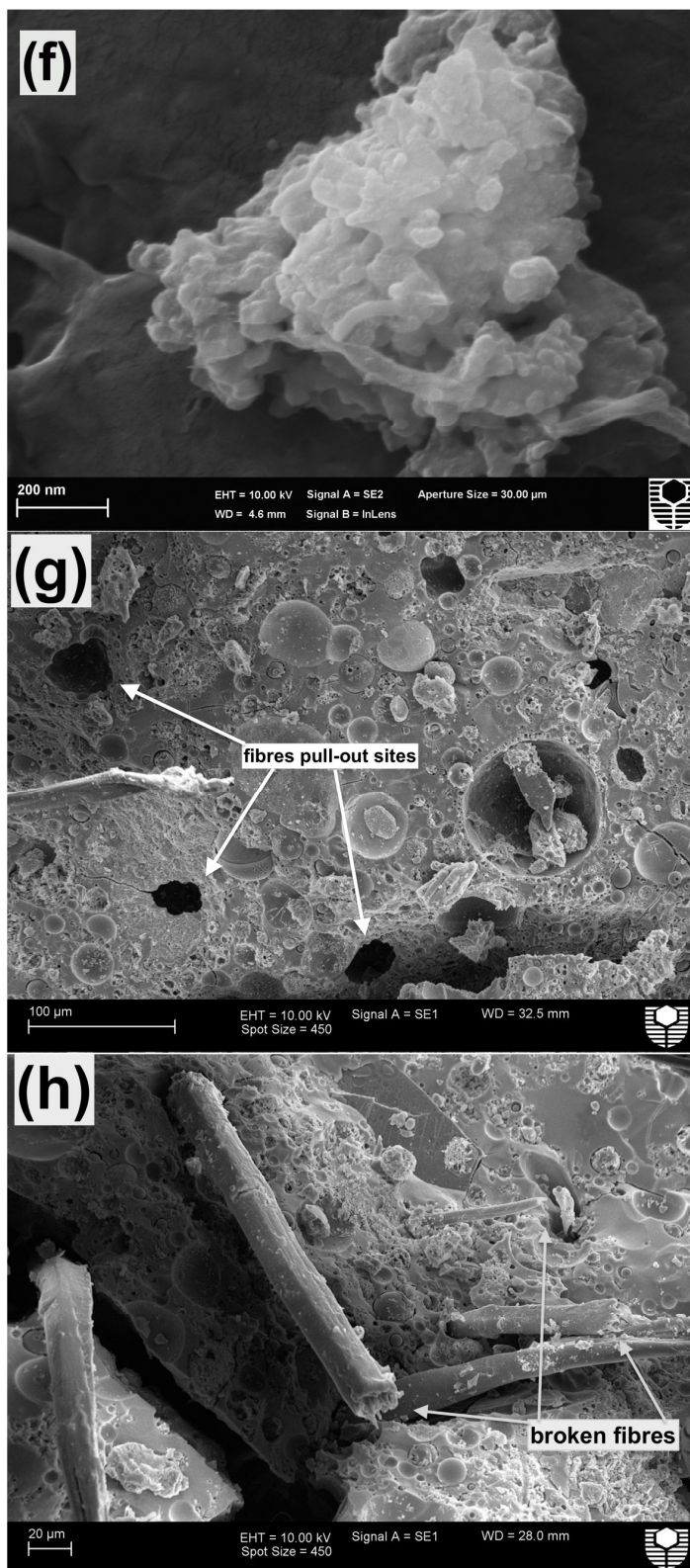
Fig. 7 (a) control sample, (b)-(d) nanocomposites containing 1- 3 wt% nanoclay, (e)-(f) agglomerated nanoparticles embedded in GPNC-3 matrix, (g) fibres pullout at GPFNC-1, (h) fibres fracture at GPFNC-2 and good adhesion bond

V. CONCLUSION

The study of geopolymer nanocomposites with FF reinforcement and effects of nanoclay on the physical and mechanical properties displayed a number of results. The FTIR showed nanocomposites of geopolymer loaded with nanoclay created higher amounts of geopolymer gel. Nanoclay added in nanocomposites at 2.0 wt% displayed a denser microstructure, and showed bond between matrix and FF to be stronger. The amount 2.0 wt% nanoclay in nanocomposites caused a reduction in porosity while increasing density. The reaction improved the flexural strength and toughness of the samples. However, an adverse reaction in the mechanical and physical property was observed in FF-reinforced geopolymer that contained more than the optimum amount of 2.0 wt%. nanoclay.

REFERENCES

[1] V. F. Barbosa, K. J. D. MacKenzie, C. Thaumaturgo, "Synthesis and characterisation of materials based on inorganic polymers of alumina and silica: sodium polysialate polymers," *Int. J. Inorg. Mater.*, vol. 2, pp. 309-17, 2000.

[2] F. J. Silva, C. Thaumaturgo, "Fibre reinforcement and fracture response in geopolymeric mortars," *Fatigue. Fract. Eng. Mater. Struct.*, vol. 26, no. 2 SPEC., pp. 167-72, 2003.

[3] Q. Zhao, B. Nair, T. Rahimian, P. Balaguru, "Novel geopolymer based composites with enhanced ductility," *J. Mater. Sci.*, vol. 42, pp. 3131-7, 2007.

[4] A. Hakamy, F. U. A. Shaikh, I.M. Low, "Thermal and mechanical properties of hemp fabric-reinforced nanoclay–cement nanocomposites" *J. Mater. Sci.*, vol. 49, pp. 1684-94, 2013.

[5] C. A. U. Shanshan, H. Wang, X. Wang, "Chemical and Mechanical Properties Studies of Chinese Linen Flax and its Composites," *Poly. Poly. Compos.* vol. 21, pp. 275-85, 2013.

[6] H. Assaedi, F. U. A, Shaikh, I. M. Low, "Characterisation of mechanical and thermal properties in flax fabric reinforced geopolymer composites," *J. Adv. Cer.*, submitted for publication.

[7] T. Phoo-ngernkham, P. Chindaprasirt, V. Sata, S. Hanjitsuwan, S. Hatanaka, "The effect of adding nano-SiO_2 and nano-Al_2O_3 on properties of HVFA geopolymer cured at ambient temperature," *Mater. Des.*, vol. 55, pp. 58-65, 2014.

[8] A. Nazari, J. G. Sanjayan, "Hybrid effects of alumina and silica nanoparticles on water absorption of geopolymers: Application of Taguchi approach," *Measurement*, vol. 60, pp. 240-6, 2015.

[9] M. Saafi, Andrew K., Tang P. L., McGhon D., Taylor S., Rahman M., et al., "Multifunctional properties of carbon nanotube/fly ash geopolymeric nanocomposites, "*Constr. Build. Mater.*, vol. 49, pp. 46-55, 2013.

[10] F. U. A. Shaikh, S. W. M. Supit, "Mechanical and durability properties of high volume fly ash (HVFA) concrete containing calcium carbonate ($CaCO_3$) nanoparticles," *Constr. Build. Mater.*, vol. 70, pp. 309-21, 2014.

[11] ASTM C20, "Standard test methods for apparent porosity, water absorption, apparent specific gravity, and bulk density of burned refractory brick and shapes by boiling water", 2010.

[12] ASTM D790, "Standard Test Methods for Flexural Properties of Unreinforced and Reinforced Plastics and Electrical Insulating Materials," 2010.

[13] A. Fernandez-Jimenez, Palomo A., "Composition and microstructure of alkali activated fly ash binder: Effect of the activator," *Cem Concr Res*, vol. 35, no. 10, pp. 1984-92, 2005.

[14] T. Alomayri, I.M. Low, "Synthesis and characterization of mechanical properties in cotton fiber-reinforced geopolymer composites," *J. Asian Ceram. Soc.*, vol. 1, no. 1, pp. 30-4, 2013.

[15] N.C. Tanw, A.v. Riessen, "Determining the Reactivity of a Fly Ash for Production of Geopolymer," *J. Amer. Ceram. Soc.*, vol. 92, pp. 881-7, 2009.

[16] T. Bakharev, "Thermal behaviour of geopolymers prepared using class F fly ash and elevated temperature curing," Cem Concr Res, vol. 36, no. 6, pp. 1134-47, 2006.

[17] W. D. A. Rickard, R. Williams, J. Temuujin, A.v. Riessen, "Assessing the suitability of three Australian fly ashes as an aluminosilicate source for geopolymers in high temperature applications," Mater Sci Eng., vol. 528, no. 9, pp. 3390-7, 2011.

[18] J. W. Phair, J.S.J. Deventer, "Effect of the silicate activator pH on the microstructural characteristics of waste-based geopolymers," *Int. J Miner. Process.*, vol. 66, no. 1-4, pp. 121-43, 2002.

[19] E. ul-Haq, S. K. Padmanabhan, A. Licciulli, "Synthesis and characteristics of fly ash and bottom ash based geopolymers–A comparative study," *Ceram. Int.*, vol. 40, no. 2, pp. 2965-71, 2014.

[20] T. Alomayri, H. Assaedi, F. U. A. Shaikh, I. M. Low, "Effect of water absorption on the mechanical properties of cotton fabric-reinforced geopolymer composites," *J Asian Ceram. Soc.*, vol. 2, pp. 223-30, 2014.

[21] F. Shaikh, S. Supit, P. Sarker, "A study on the effect of nano silica on compressive strength of HVFA mortars and concretes," *Mater. Des.*, vol. 60, pp. 433-42, 2014.

[22] M. Alzeer, K. MacKenzie, "Synthesis and mechanical properties of novel composites of inorganic polymers (geopolymers) with unidirectional natural flax fibres," *App. Clay Sci.*, vol. 76, pp. 148-52, 2013.

[23] J. Sim, C. Park, D.Y. Moon, "Characteristics of basalt fiber as a strengthening material for concrete structures," *Compos. B*, vol. 36, no. 6-7, pp. 504-12, 2005.